Experiments on a Bearingless Synchronous Reluctance Motor with Load

MORI Satoshi, SATOH Tadashi, OHSAWA Masaru

Dynamics Research Dept., Center for Fluids and Mechanical Engineering,
Ebara Research Co.,LTD.
4-2-1,Hon-Fujisawa, Fujisawa, Kanagawa Pref. 251, Japan.
Phone: +81-466-83-7645,Fax: +81-466-82-9371, e-mail: mori05558@erc.ebara.co.jp

Abstract: A prototype of a synchronous reluctance type, magnetically-levitated motor system was developped and tested. This sytem is built with a horizontal configraton. The rotor of the system is non-contact-levitated by two bearingless motors. In a non-load operation, the axial directon is supported by a passive stiffness which is consequent to these motors. Four poles of each bearingless motor were set as magnetic poles for the drive (torque), while two poles of the same were set as those for the control (radial force). Static load characteristics of the bearingless motors were measured using both magnets for the radial load and force sensors, set at both ends of the shaft. It was confirmed that the system was capable of rotation at 12,000 rpm under a non-torque-load state. A torque load was applied by a DC generator and measured by a torque meter, connected by a flexible coupling, and an output of 2.12 kW was confirmed at 8,000 rpm. Measurement was also made on the vibration amplitude of the rotor by changing the phase lag of the magnetic flux for drive versus the one for control. The following discusses experimental results and considerations.

1 Introduction

Consistent development is underway these years on the design and control of magnetic bearings which are in demand for various rotating machinery. This is because magnetic bearings carry advantages, as compared with conventional contact type baerings, such as higher rpm due to the non-contact support of the rotor, easier maintenance, and better electric controllability of bearing characteristics.

When we look at rotating machines equipped with magnetic bearings, we find that almost all include motors for driving the rotor. The structural elements of such motors are identical to that of magnetic bearings which constitute magnets and coiles. Accordingly, it is logical to consider a levitation type, rotating machine whose motor and magnetic bearings constitute an integrated structure. Such an integrated configration allows the mechanism of motors to be aligned with that of the magnetic bearings; an overall compactness, including control elements, can be realized. Consequently, the rotor operation can be more stable and rotated at higher speed. As such type of rotating machine does not have an established name, we shall hereon refer to it a BELM (Bearingless Motor).

Some reports are available on systems such as the BELM [1] [2]. However, no such reports touch on load test results of a case where only a BELM is used for complete levitation. The following discusses one such attempt, whereby radial and torque load tests were carried out using a 4-pole, synchronous, reluctance type horizontal setup BELM prototype. Its pole number for the motor (torque generation) was four, while that for its radial force was two.

2 Experimental apparatus

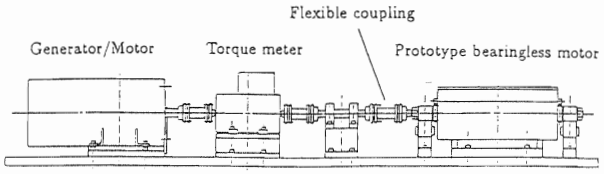

Fig.1 Experimental setup

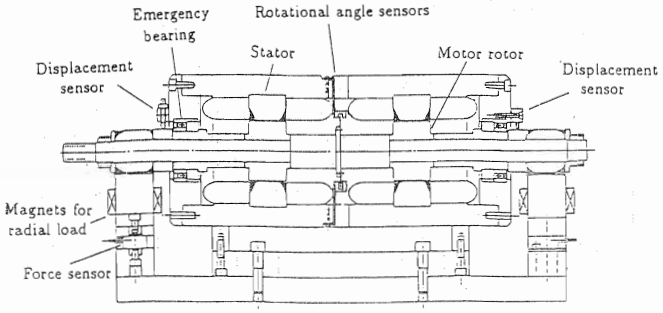

Fig.2 Prototype bearingless motor with 4 axis control

Figure 1 shows a structual diagram of the experimantal apparatus, while Figure 2 shows a cross-sectional diagram of the prototype BELM. The rotor was supported by two BELMs, one end of which was connected to a torque meter by a flexible coupling. The other end of the torque meter was connected to a DC generator/motor by flexible coupling. The torque load was controlled by adjusting the electric current supplied to the field winding of the generator. Electoromagnets were installed at both ends of the rotor to generate vertically-downwoard load by magnetic force. This magnetic force applying on the rotor as a load was measured by force sonsors installed between the load magnetic poles and base. A detection

plate and photo interrupter, for detecting the rotational angle of the rotor, were installed between two BELMs. As indicated in the diagram, displacement sensors, for detecting the vertical and horizontal displacement, were installed at both side of test equipment, and emergency bearings were also installed in same location. The radial clearance between the emergency bearing and the rotor was 0.15 mm.

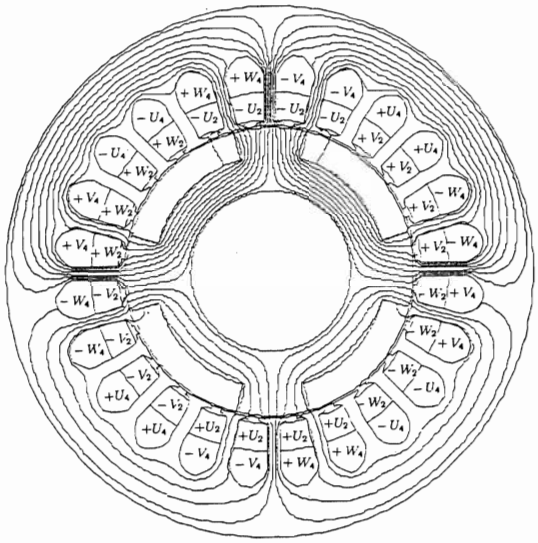

Fig.3 Radial force production

Figure 3 shows the cross-sectional configration of the BELM, including the magnetic flux lines calculated by FEM. The rotor was made from carbon steel for structual use (S15C), while the stator constituted laminated layers of regular silicon steel plates. The outer diameters of the rotor was 72 mm, while the inner diameter of the stator was 73 mm. The bearing clearance was therefore 0.5 mm. The width of both the rotor and the stator was identical at 45 mm. The weight of the rotor was 9.5 kg. The characters indicated at the stator slot represent windings. The characters indicated at the outer side of the slot represent a 4-pole winding arrangement, while those at the inner side of the same represent a 2-pole winding arrangement. As acknowledged form the figure, both 2-pole and 4-pole windings were constituted 3-phase arrangement, and wound on an identical stator slot. The analytic parameters for magnetic flux indicated in the figure, were magnetizing current supplied to 4-pole winding $I_d = 7.5A$, and control current for radial force production supplied to 2-pole windings 4.4 A, which were measued value when the rotor was levitated with the gravitational load of the rotor mass. Magnetic flux was concentrated on the upper side of the rotor, the magnetic force applying on the rotor in the vertical direction. Here, the magnetic flux density became gratest at the teeth on the upper side of the stator (1.17 T, in this case).

Figure 4 shows a block diagram of the rotational / levitational control system. A synchronization between the rotational and levitational systems is made at the rotation angle of the rotor ωt . In the rotational control system, a negative feedback was made by observing rotational speed ω . Torque current command I_q^* was generated by PI controller which input was the error of the rotational speed. The generated torque current commnad and pre-determined magnetizing current command I_d^* were transformed to 2-phase coil current commands i_a^* and i_b^*, and further they were transformed to 3-phase current command i_{U4}^*, i_{V4}^* and i_{W4}^* . These signals were amplified by current amplifiers and electric currents for rotation supplied to 4-pole windings.

In case of the levitational system, displacement of the rotor in α (horizontal) direction and β (vertical) direction were used negative feedback signals. Control force commands F_α^* and F_β^* were generated by PID controllers which inputs were each errors. Control force commands were transformed to 2-phase coile current commands i_α^* and i_β^*, synchronized to the rotation angle of the rotor. In similar way described above, electric currents for levitation i_{U2}^*, i_{V2}^* and i_{W2}^* supplied to 2-pole windings. Phase θ, in the transformation of Control force commands and 2-phase coil current commands, indicated a phase lag between them. This phase hereinafter be called the control-phase angle. As for the principle of levitation in regard to a BELM with this mechanism, and other relevant topics, minute decription was found in privious reports [1] [2] [3] [4].

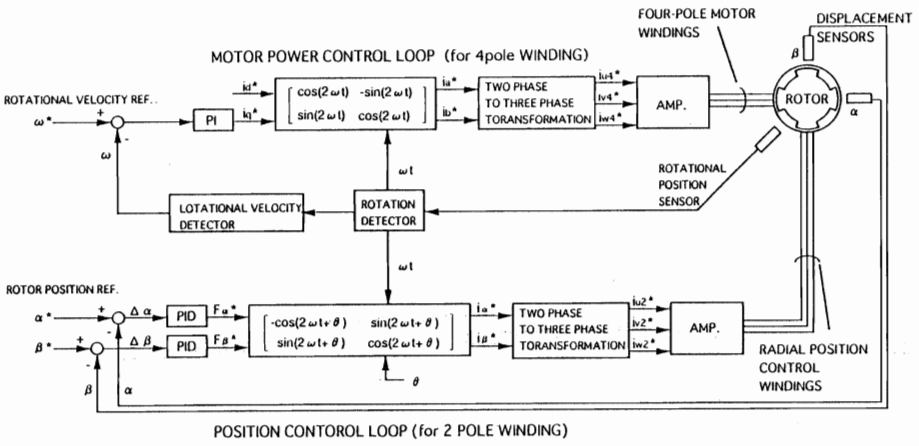

Fig.4 Block diagram of the control system

3 Experimental Results and Considerations

3.1 Stiffness of BELM

As for measuring the stiffness of BELM as magnetic bearing, the magnetic force and the radial displacement were measued by causing the magnetic force to affect the rotor using the electromagnet for load. Only the vertical direction (β direction) was measured. Accordingly, not only the gravitational weight of the rotor, but also magnetic force due to the electromagnet for load affected the rotor.

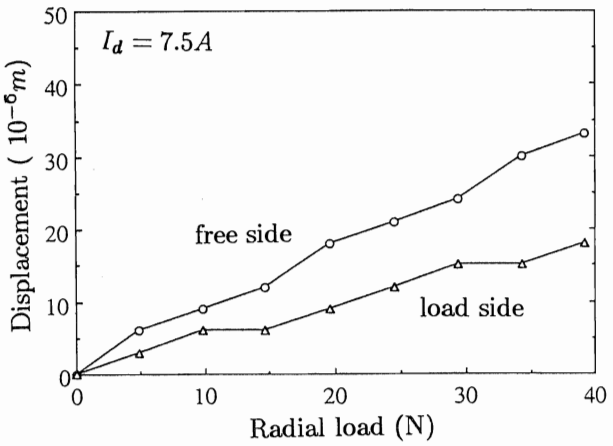

Fig.5 Radial load and displacement

Figure 5 shows variations in the displacement in β direction versus the magnetic force applied as a load. The magnetizing current I_d , supplied to 4-pole windings, was set as 7.5 A. The bearing stiffness of each BELM installed load side and free side, indicated approximately $2 \times 10^6 N/m$ and $1 \times 10^6 N/m$, respectively. The difference between these measued values may caused by controller gain settings. And these results indicated values which were not inferior to those of a conventional magnetic bearing. Considering the gravitational weight of the rotor, the maximum load rating here was 87 N.

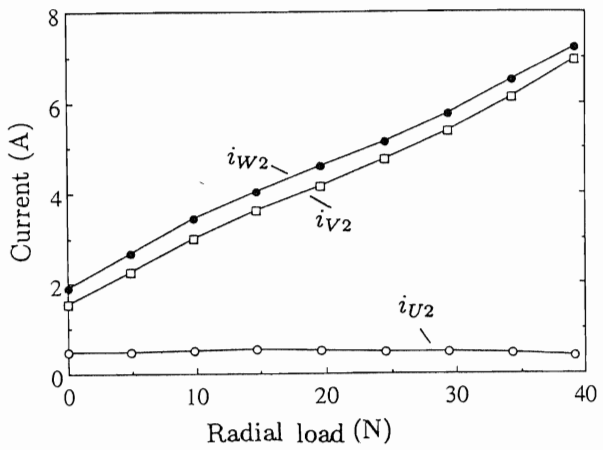

Fig.6 Currents of 2-pole winding and radial load

Figure 6 shows variations in electric currents of the 2-pole windings in the BELM installed free side versus radial load in same condition described above. A linear increase in the electric current is shown along the increase in load. There were no variations in the U-phase electric current i_{U2}, as the mechanical rotation angle of the rotor was set, in this case, as zero degree. It was clarified that the radial force was linearly varied by the current in 2-pole windings due to the existence of the magnetizing current like a conventional magnetic bearing.

3.2 Torque Load Test

The vibration of the rotor, when a torque load was applying, was measured while maintaining the rpm at a constant. The rotor was connected to a torque load by a flexible coupling. Control of the torque load was done by adjusting the field current of the DC generator.

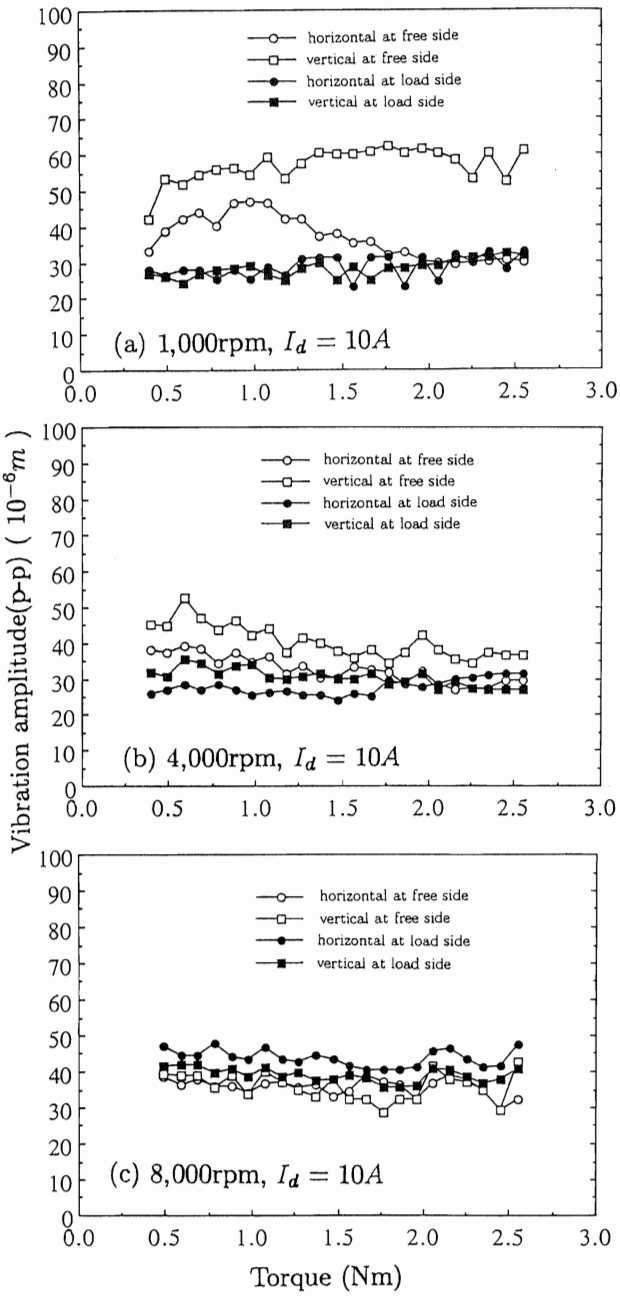

Fig.7 Vibration amplitude(p-p) and torque load

The rpm was adjusted, to maitain a constant, while measuring the torque load by torque meter.

Figure 7a, b and c show the relationship between vibration amplitude (peak to peak) of the rotor and torque at 1,000 rpm, 4,000 rpm and 8,000 rpm, respectively. A torque load exceeding 2.55 Nm was not applied as the 4-pole windings became heated, caused by inclease of a torque current. Thus an rpm of 8,000 and a torque load of 2.55 Nm were not critical conditions and there was a possibility of higher rpm and torque load. As acknowledged from figure, there was no significant change in the vibrational displacement of the rotor along an increase in the torque load. On the contrary, there was a decreese in the vibration amplitude of the free-end of the rotor. The vibration amplitude of the rotor, measured in this experiment, was from $30\mu m$ to $50\mu m$. And the greatest output was 2.12 kW at 8,000 rpm, under magnetizing current $I_d = 10A$.

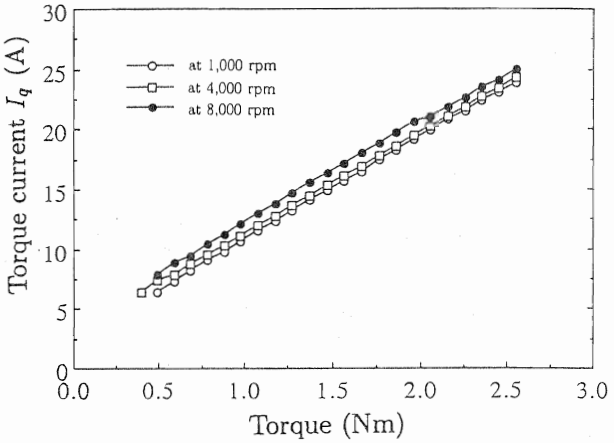

Fig.8 Torque current I_q and torque load, $I_d = 10A$

The relationship between torque current I_q and the torque load was studied.Figure 8 shows variations in the torque current I_q versus the torque load when the magnetizing current I_d was 10 A. It was found that the torque current increased proportional to an inclease in the torque load. From the observation that the linearity did not change at the maximum torque load of 2.55 Nm, it is speculated that a greater torque load could be generated. The amplitude of the torque current at maximum torque load was 25 A.

The control-phase angle θ in the conversion between the the radial force command and the control current command, indicated in the BELM control block diagram (see Figure 2), have great effect on the stable control of the BELM. The rotor vibration amplitude was measured to clarify this effect during a levitated rotation, under a torque load, with one BELM unit in operation, and with variations in the control phase angle θ.

Figure 9a, b, c and d are results of measurements made on rotor vibration versus the control-phase angle, with the magnetizing current I_d at 7.5 A and the rotor rpm at 1,000 rpm. Appropriate control-phase angles, for maintainig a stable rotor levitation, depending on torque load values, were confirmed. The critical value of the control-phase angle, insofar as the present prototype BELM is concerned and under the above conditions, was found to be 20 degrees.

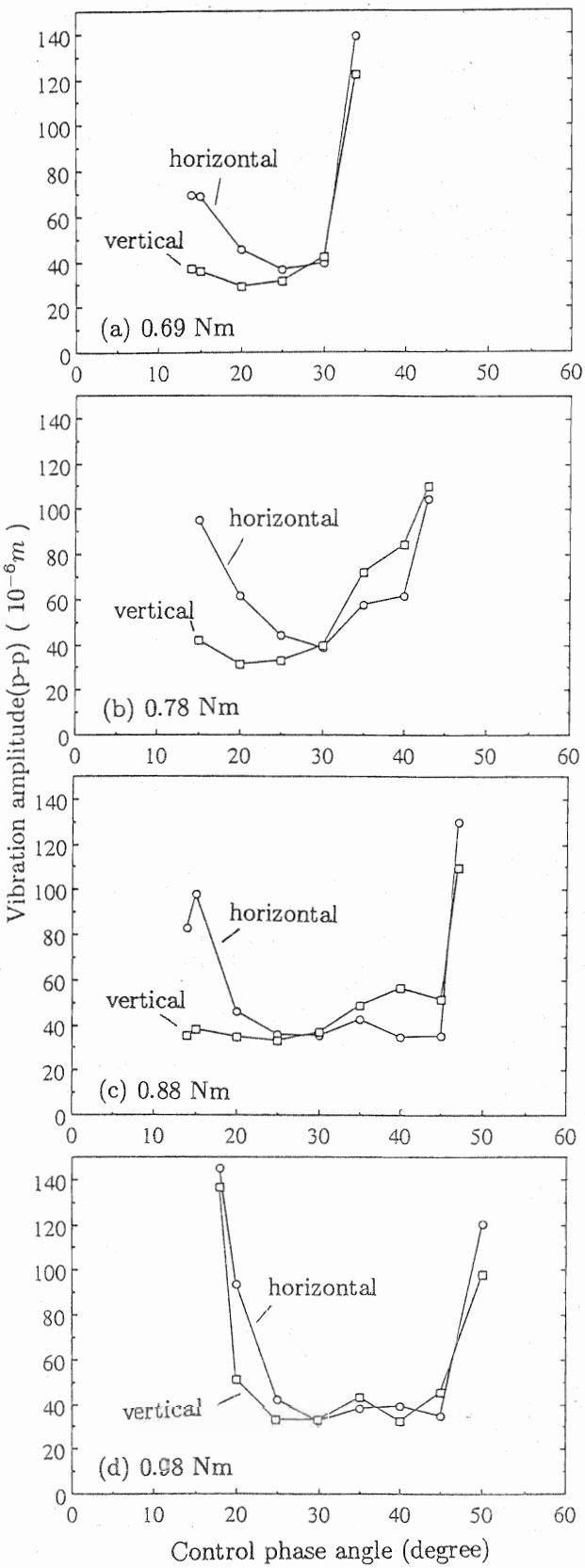

Fig.9 Vibration amplitude(p-p) and control phase angle at 1,000 rpm $I_d = 7.5A$

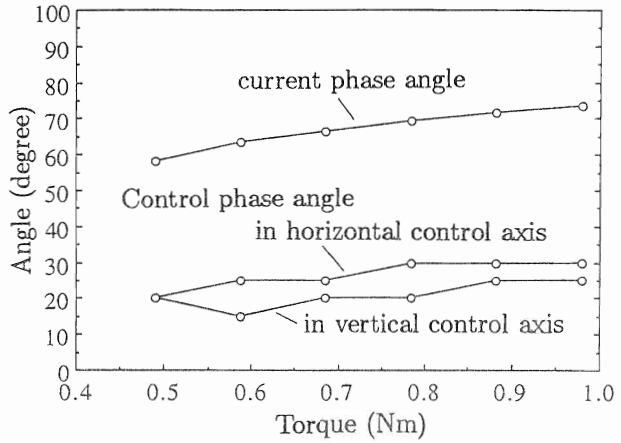

Fig.10 Stable control phase angle and torque load ($I_d = 7.5A$) at 1,000 rpm

Figure 10 shows the relationship between the control-phase angle and the torque load, under the same conditions as mentioned above, for minimizing rotor vibration. Also shown in the figure is the current-phase angle $\varphi = \tan^{-1}(\frac{I_q}{I_d})$. The current-phase angle increased along an increase in the torque load, and the control-phase angle showed an identical tendency to increase as well. Under a torque load of 0.49 Nm, the control-phase angle was 20 degrees, while the current-phase angle was 58 degrees. Under a torque load of 0.98 Nm, the control-phase angle was 30 degrees, while the current-phase angle was 73 degrees.

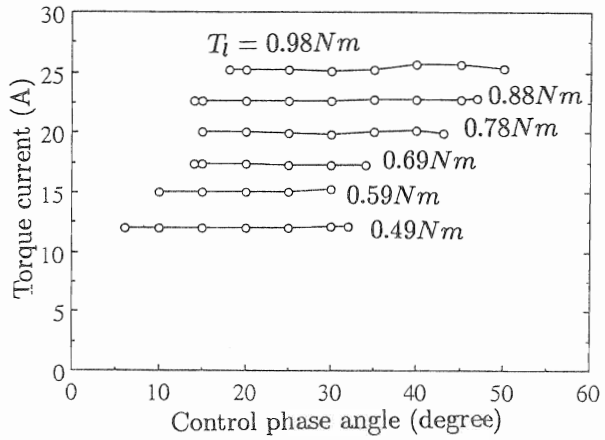

Fig.11 Torque current and cotrol phase angle at 1,000 rpm ($I_d = 7.5A$)

Figure 11 shows the relationship between the control-phase angle and torque current, for each torque load. The torque current was found not to depend on the control-phase angle, and to be at a constant when the torque load was at a constant.

4 Conclusions

A 4-axis control, synchronous type, reluctance bearingless motor was levitated completely using horizontal setup and its operation at 12,000 rpm under no load was confirmed. The bearing stiffness of the prototype BELM was approximately $1 \sim 2 \times 10^6$ N/m, which was identical to that of conventional magnetic bearings. A stable critical value (about 20 degrees at 1,000 rpm) of the control-phase angle was found depending on the torque load. And the value of the stable control-phase angle showed a tendency to increase along an increase in the current-phase angle consequent to an increase in the generated torque. But the control-phase angle had no influence on the generated torque.

References

[1] Akira Chiba, M. Azizur Rahman and Tadashi Fukao, "Radial Force in a Bearingless Reluctance Motor", IEEE trans vol.27, pp.786-790, 1991.

[2] Yohji Okada, Seiji Shimura and Tetsuo Ohishi, "Horizontal Experiments on a PM Synchronous Type and Induction Type Levitated Rotating Motor", IPEC Yokohama, pp.340-345, 1996.

[3] Osamu Ichikawa, Chikara Michioka and Tadasi Fukao, "A Decoupling Control Method of Radial Rotor Positions in Synchronous Reluctance Type Bearingless Motors", IPEC Yokohama, pp.346-351, 1995.

[4] M.Azizur Rahman, Tadashi Fukao and Akira Chiba, "Principles and Developments of Bearingless AC Motors", IPEC Yokohama, pp.1334-1339, 1995.